CO-PRIME CIRCULAR MICROPHONE ARRAYS AND THEIR APPLICATION TO DIRECTION OF ARRIVAL ESTIMATION OF SPEECH SOURCES

Jiahong Zhao and Christian Ritz

School of Electrical, Computer and Telecommunications Engineering, University of Wollongong, Northfields Avenue, Wollongong, NSW 2522, Australia
E-mail: jz262@uowmail.edu.au and critz@uow.edu.au

ABSTRACT

This paper proposes the co-prime circular microphone array (CPCMA), which applies co-prime array theory to circular microphone arrays. Compared with a conventional uniform circular array (UCA) with the same number of microphones and radius, the CPCMA achieves beampatterns with a narrower main lobe and fewer side lobes, whilst also avoiding spatial aliasing, thus having no grating lobes above the Nyquist frequency of the UCA. Array gain (AG) results indicate that the CPCMA is better than the UCA at amplifying the desired target signal while suppressing noise from other directions for typical speech signal frequencies. Compared with a UCA with similar performance and the same spatial Nyquist frequency, the CPCMA significantly reduces the required number of microphones. Simulations also indicate advantages of the CPCMA in speech source DOA estimation under high noise and low reverberation, especially when there are simultaneous multiple sources.

Index Terms— Co-prime circular microphone arrays, spatial aliasing, array gain, direction of arrival estimation, speech processing.

1. INTRODUCTION

Microphone arrays and appropriate signal processing algorithms can be applied together to provide solutions for numerous problems in acoustics, including estimating the incoming direction of the sound source, source separation and decreasing the undesirable effects of noise and reverberation [1], [2]. Different structures of microphone arrays have been designed and the related applications have attracted significant research interests, such as sound localisation [3], [4], noise reduction [5] and dereverberation [6], [7], [8], [9].

Recently, the circular differential microphone array (CDMA) was proposed, targeting applications such as 3D sound recording that required similar responses in all directions [10], [11]. The CDMA achieves high directional gains and frequency-invariant beampatterns, which is an advantage for broadband signals. However, the CDMA also amplifies the white noise and encounters the so-called deep-null problem in the responses of both the directivity factor (DF) and white noise gain (WNG) [11]. To deal with it, multiple rings of CDMAs were combined to form the concentric circular differential microphone array (CCDMA) [12]. By designing the robust steerable frequency-invariant beampattern, this approach mitigates the deep-null problem.

To further address the white noise amplification, a larger number of microphones and a bigger array spacing are preferable [11]. While this may lead to an impractical number of microphones to avoid spatial aliasing, a co-prime microphone array (CPMA) [13] avoids spatial aliasing by interleaving two (much smaller) sub-arrays, where the number of microphones of each sub-array are co-prime related. Combining the beamforming outputs of each sub-array achieves improved beampatterns and hence more accurate results for applications such as broadband direction of arrival (DOA) estimation when compared to a conventional ULA with the same number of microphones and identical aperture size [14]. For example, the operating frequency (spatial Nyquist frequency) of a 16-element ULA with an aperture of 0.9 m is approximately 2.9 kHz, compared with approximately 12.3 kHz for a CPMA with the same number of elements and aperture size (the ULA would need 72 elements to achieve the same operating frequency as this CPMA).

Wideband DOA estimation for CPMAs includes the use of a model-based Bayesian framework to determine the number of sound sources [15] and group sparsity to lower the computational complexity [16]. Recent work has applied the steered response power - phase transform (SRP-PHAT) method to CPMA recordings to estimate the DOA of speech sources, which achieved more accurate DOA estimates than a ULA of the same size [17]. In comparison to this previous work, this paper proposes the co-prime circular microphone array (CPCMA), which is formed by interleaving two uniform circular arrays (UCAs) that are arranged according to the co-prime array theory. This design makes use of advantages of the CPMA in achieving improved beampatterns and array gain without requiring much large number of microphones.

Section 2 of this paper describes the mathematical model for CPCMA recordings and analyses the resulting

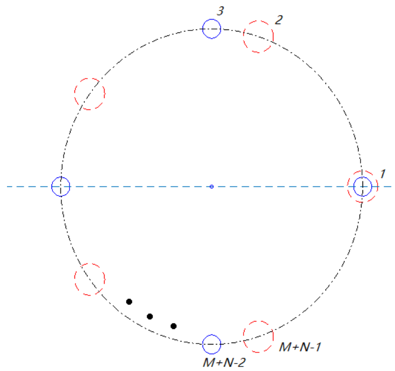

Fig. 1. An 8-element co-prime circular microphone array arrangement

beampatterns to determine the array gain. Section 3 introduces the proposed DOA estimation approach, which is based on statistical analysis of histograms of DOA estimates formed from SRP-PHAT responses derived from the CPCMA. Results for different testing scenarios are presented in Section 4 with conclusions provided in Section 5.

2. CO-PRIME CIRCULAR MICROPHONE ARRAYS AND PERFORMANCE MEASUREMENTS

2.1. Signal Model

A CPCMA interleaves two sparse uniform circular sub-arrays (see Fig. 1). The numbers of microphones in each subarray, M and N, are a pair of co-prime numbers, where the only positive integer that divides both is one. This paper assumes $N = M + 1$, which minimises the required number of elements to construct an expected array aperture [18]. The rightmost element is considered as the reference microphone shared by the two overlapped sub-arrays, thus forming a CPCMA with $L = M + N - 1$ microphones. Assuming there are K uncorrelated narrowband (or wideband) sound sources that propagate at the speed of sound ($c = 343$ m/s), leading to plain waves impinging on the CPCMA from different DOAs θ_i ($i = 1, 2, \dots, K$), the mathematical model of the CPCMA recording can be formulated as

$$\boldsymbol{y}(t) = \boldsymbol{h}(t) * \boldsymbol{s}(t) + \boldsymbol{v}(t) \quad (1)$$

where $\boldsymbol{y}(t) = [y_1(t), \dots, y_L(t)]^T$ is the output of the CPCMA, and $\boldsymbol{s}(t) = [s_1(t), \dots, s_K(t)]^T$, $\boldsymbol{h}(t) = [h_1(t), \dots, h_L(t)]^T$ and $\boldsymbol{v}(t) = [v_1(t), \dots, v_L(t)]^T$ represent source signals, acoustic impulse responses from the source signals to microphones and additive noise, respectively. The noise at each microphone is assumed to be uncorrelated and of the same power.

Assuming the reference microphone of the CPCMA is configured on the x axis, for plain wave sound sources the time delay between the ith microphone and the centre is [11]

$$\tau_i = \frac{r}{c}\cos(\theta - \varphi_i), i = 1, 2, \dots, L \quad (2)$$

where r is the radius of the CPCMA, and

$$\varphi_i = \begin{cases} \frac{2\pi \cdot \frac{i}{2}}{N} = \frac{\pi i}{N}, & i \bmod 2 = 0 \\ \frac{2\pi(\frac{i+1}{2} - 1)}{M} = \frac{\pi(i-1)}{M}, & i \bmod 2 = 1 \end{cases} \quad (3)$$

is the angular location of the ith microphone. In this way, the steering vector of length L is

$$\begin{aligned} \boldsymbol{d}(\omega, \theta) &= [e^{j\omega\tau_1} \quad \dots \quad e^{j\omega\tau_L}]^T \\ &= [e^{j\omega r c^{-1}\cos(\theta - \varphi_1)} \quad \dots \quad e^{j\omega r c^{-1}\cos(\theta - \varphi_L)}]^T \end{aligned} \quad (4)$$

where the superscript T represents the transpose operation, $j = \sqrt{-1}$ is the imaginary unit, and $\omega = 2\pi f$ is the angular frequency for temporal frequency f. The wavelength of the sound source is $\lambda = c/f$, and the spacing between the i_1th and i_2th microphone ($i_1 - i_2 = 1$) is

$$\delta_{i_1 i_2} = \begin{cases} 2r\sin\left(\frac{\pi i_1}{2N} - \frac{\pi(i_2-1)}{2M}\right), & i_1 \bmod 2 = 0 \\ 2r\sin\left(\frac{\pi(i_1-1)}{2M} - \frac{\pi i_2}{2N}\right), & i_1 \bmod 2 = 1 \end{cases} \quad (5)$$

According to the spatial Nyquist sampling theorem, for ULAs, if the inter-element spacing δ' is greater than half of the wavelength λ', i.e. $\delta' > \lambda' / 2$, there will be spatial aliasing. This results in multiple grating lobes in the beampattern, which have the same power level as the main lobe, thus degrading the performance for applications such as DOA estimation. For a UCA, the operating frequency f_{op_UCA}, below which spatial aliasing will not occur, can be found as follows [11].

$$f_{op\_UCA} = \frac{c}{2\delta'} = \frac{c}{4r'\sin\left(\frac{\pi}{M'}\right)} \quad (6)$$

where r' and M' are the radius and number of microphones. For a co-prime microphone array, the operating frequency can be derived by replacing the number of elements in (6) with the product of the number of microphones of each sub-array and can be approximated as [14]

$$f_{op\_CPCMA} \approx \frac{c}{4r\sin\left(\frac{\pi}{M \cdot N}\right)} \quad (7)$$

2.2. Performance Measures

For a fixed beamformer, two of the most important measurements to evaluate the performance are the beampattern and the array gain [19]. The beampattern describes the sensitivity of a beamformer to a plane wave impinging on the microphone array. For a subarray of the CPCMA with I microphones, which is a normal UCA, it is formulated as [11]

$$\begin{aligned} \boldsymbol{B}[\boldsymbol{w}(\omega), \theta] &= \boldsymbol{w}^H(\omega)\boldsymbol{d}(\omega, \theta) \\ &= \textstyle\sum_{i=1}^{I} W_i^*(\omega)\, e^{j\omega r c^{-1}\cos(\theta - \varphi_i)} \end{aligned} \quad (8)$$

where the superscripts H and $*$ denote the conjugate-transpose operation and complex conjugation, respectively. Additionally, $\boldsymbol{w}(\omega)$ of length I are generally complex beamforming weights, which can be expressed as

$$\boldsymbol{w}(\omega) = [W_1(\omega) \quad W_2(\omega) \quad \cdots \quad W_I(\omega)]^T \quad (9)$$

where $W_i(\omega)$ ($i = 1, 2, \dots, I$) is the individual weight applied to each microphone signal. This paper assumes equal weights although other weights could be derived using existing beamforming techniques, thus the beampattern of the CPCMA can be achieved by combining that of the two subarrays, which is [14]

$$\boldsymbol{B}_{CPCMA} = \boldsymbol{B}_{UCA\_M} \times \boldsymbol{B}^{*}_{\boldsymbol{UCA\_N}} \tag{10}$$

where $\boldsymbol{B}_{UCA\_M}$ and $\boldsymbol{B}_{UCA\_N}$ are the beampatterns of the subarrays with M and N microphones, separately.

Another key measure for microphone arrays is the array gain (AG), which is defined as the ratio between the gain to the desired signal and the average gain to spatial noises from all undesired directions [19]. The AG can be given by

$$D[\boldsymbol{w}(\omega)] = \frac{|\boldsymbol{B}[\boldsymbol{w}(\omega),\theta_s]|^2}{1/\Theta \sum_{\theta} |\boldsymbol{B}[\boldsymbol{w}(\omega),\theta]|^2} \tag{11}$$

where θ_s is the steering angle, and Θ is the number of discrete angles used in calculating the beampattern $\boldsymbol{B}$.

3. DOA ESTIMATION USING SRP-PHAT AND HISTOGRAM-BASED STOCHASTIC ALGORITHMS

3.1. DOA Estimation Based on SRP-PHAT

For linear co-prime microphone arrays, it has been shown that SRP-PHAT method can be used accurately estimating the DOA [17]; here we derive the SRP-PHAT method for the CPCMA. The SRP value $P(\tau)$ at each incidence angle is found by summing the generalised cross-correlations (GCC) of all combinations of microphone pairs [20].

$$P(\tau) = \sum_{i_1=1}^{L} \sum_{i_2=i_1+1}^{L} \int_{-\infty}^{+\infty} \frac{\vartheta_{y_1 y_2}(f)}{|\vartheta_{y_1 y_2}(f)|} e^{j2\pi f \tau} df \tag{12}$$

where P is the SRP of the microphone array, and $\vartheta_{y_1 y_2}(f)$ is the cross-spectrum given as follows.

$$\vartheta_{y_1 y_2}(f) = E[Y_1(f) Y_2^{*}(f)] \tag{13}$$

where $E[\cdot]$ calculates the mathematical expectation, and $Y_j(f), (j = 1, 2)$ are the outputs of the selected microphone pairs in the frequency domain. Consequently, the initial DOA estimate is

$$\theta_{est} = \arccos\left(\frac{c\tau_{opt}}{|\delta_{i_1 i_2}| \cdot F_s}\right) \tag{14}$$

where F_s is the sampling frequency, and τ_{opt} is the optimal time lag leading to the largest SRP value, which is given by

$$\tau_{opt} = \underset{\tau}{\operatorname{argmax}}\big(P(\tau)\big) \tag{15}$$

3.2. Result Enhancement Algorithms

All the DOA estimates for each angle in the steering range can form a histogram, the peak of which corresponds to the source DOA. However, in noisy, reverberant or multisource scenarios, the microphones will receive many signals from undesired directions in addition to the direct source path, which results in a spreading in the histogram and thus having negative impacts on DOA estimation.

An SRP-adjusted histogram (SAH) approach can mitigate these undesired influences [17] by considering the energy of the time-frequency instants (similar to other weighting methods [21], [22]). The DOA estimation results having low SRP values are identified as insignificant to the DOA histogram, which are removed by using

$$hist_{sah}(\theta_j) = \begin{cases} hist(\theta_j) - 1, & P(\theta_j) < T \\ hist(\theta_j), & P(\theta_j) \geq T \end{cases} \tag{16}$$

where θ_j ($0^\circ \leq \theta_j \leq 180^\circ$) represents each possible DOA under consideration, $hist$ is the original histogram which counts the number of DOA estimates at each θ_j, and $hist_{sah}$ is the SRP-adjusted histogram. In addition, P is determined from (12), and T is a pre-defined energy threshold.

Although the SAH improves the accuracy of DOA estimation by being sensitive to high-energy contributors only, there can be discrete angles with higher energy than the true sources due to significant levels of noise and reverberation, leading to less distinguishable histogram peaks. To further increase the accuracy, a stochastic algorithm based on kernel density estimation (KDE) [23] is utilised to search for the local maximum of the probability density function (PDF) of the SAH [17]. The density function used in KDE can be expressed as [24]

$$\hat{f}(x) = \frac{1}{nh} \sum_{k=1}^{n} U\left(\frac{x - x_k}{bw}\right) \tag{17}$$

where U is a pre-defined kernel function, bw ($bw > 0$) is the bandwidth which can smooth the PDF curve, x_k ($k = 1, 2, \dots, n$) is an evenly distributed sample, and f is the distribution of x. The final optimised DOA estimates are found as the peaks of this PDF.

Table 1. Experimental Microphone Array Configurations

Type of array	Number of elements	Radius (m)	f_{op} (Hz)
CPCMA	8	0.12	4567.9
UCA8	8	0.12	1867.3
UCA20	20	0.12	4567.9

Table 2. Experimental Settings

Sampling frequency (F_s)	8 kHz
Frequency bin number for FFT	200
Frame duration	25 ms
Frame overlap	50%
Number of frames	180
Azimuthal range	0˚ - 180˚
Azimuthal resolution	0.1˚
Room dimensions	$8 \times 9 \times 4\ m^3$
Reverberation time (RT60)	{0, 200} ms
Noise Levels (SNRs)	{-10, 0, 10, 20, 30, 40} dB
Ground truth DOAs (S_1, S_2, S_3)	{114.8˚, 82.0˚, 69.6˚}
Source-array distance	7.2 m
Speed of sound (c)	343 m/s

4. RESULTS AND DISCUSSION

4.1 Experimental Setup

As shown in Table 1 and 2, a CPCMA and two contrastive UCAs (UCA8 with 8 elements and UCA20 with 20 elements) with the same radius are simulated in a room, and the

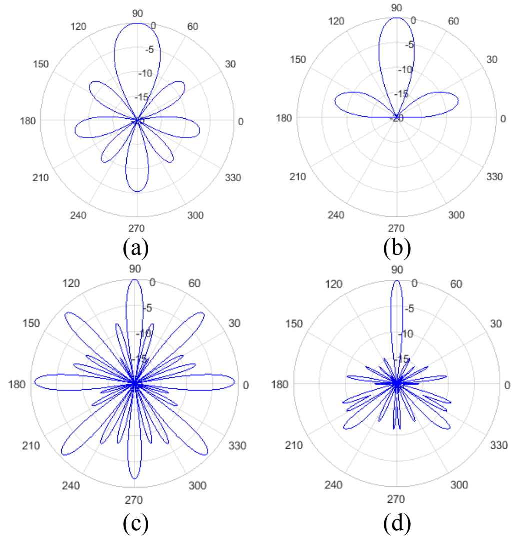

Fig. 2. Beampatterns of the 8-element UCA and CPCMA: (a) UCA at 2 kHz, (b) CPCMA at 2 kHz, (c) UCA at 6 kHz, and (d) CPCMA at 6 kHz source frequencies. Conditions of simulation: $\theta_s = 90^{\circ}$.

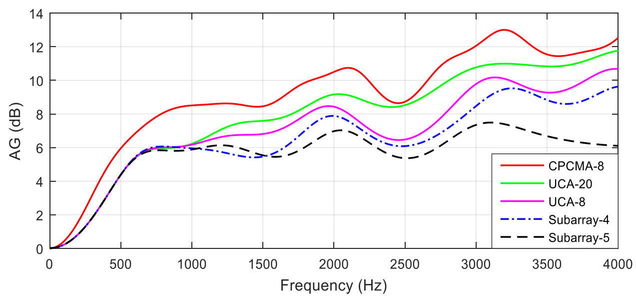

Fig. 3. Comparison of AGs of the UCAs and CPCMA. Conditions of simulation: $\theta_s = 90^{\circ}$.

speech recordings are obtained by utilising the IMAGE method [25]. Speech utterances are selected from the IEEE corpus [26] and the NOIZEUS corpus (clean sources) [27], and all sources are of the same distance from the centre of the arrays and located in three fixed positions in the far field. Recorded signals are transformed to the short-term frequency domain by applying the Fast Fourier Transform (FFT) using 50% overlapped Hamming windowed frames of 25 ms duration. DOA estimates are achieved based on SRP-PHAT and SAH technique of Section 3.2. One set of three-speech mixtures are analysed to find the average DOA estimation error using the root mean square error (RMSE), given by $RMSE = \sqrt{\frac{1}{H}\sum_{k=1}^{H}(\theta_k - \theta_{true})^2}$, where H is the number of estimates, θ_k $(k = 1, 2, \ldots, H)$ are the DOA estimation results, and θ_{true} are ground truth DOAs. Different levels of additive (white) noise and reverberation are also considered.

4.2 Co-prime Beamformer Performance

Figure 2 shows plots of beampatterns of the 8-element UCA and CPCMA (see Table 1) at 2 kHz and 6 kHz, respectively. As can be seen, the CPCMA has a narrower main lobe and fewer side lobes than the UCA at both frequencies. In addition, there are no grating lobes and only small side lobes in the CPCMA beampatterns, which indicates advantages in recording high-frequency components of broadband signals.

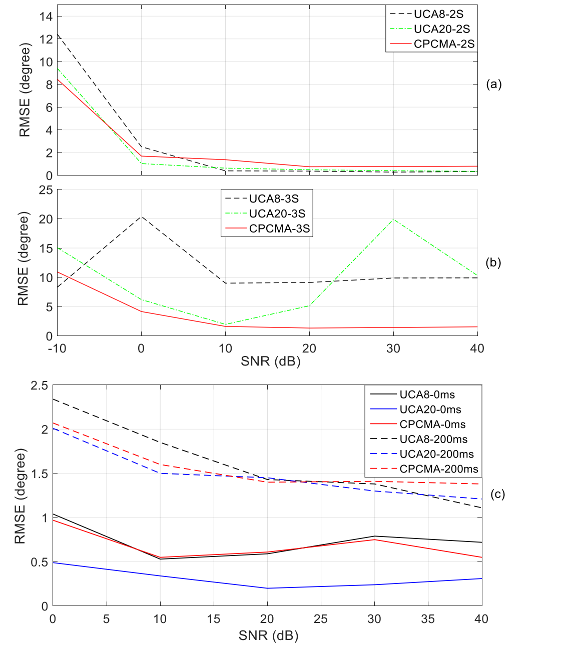

Fig. 4. Comparing SAH-based DOA estimation results for the 8-element UCA, 20-element UCA and CPCMA under different numbers of speech sources and multiple levels of noise and reverberation.

Figure 3 plots AGs of the UCAs, CPCMA and two subarrays of the CPCMA. It can be seen that the AG of the CPCMA increases significantly compared to the other four UCAs. For example, at 1kHz, there is about a 2.5 dB elevation in the gain of the CPCMA.

Figure 4 considers three types of microphones (see Table 1), where (a) and (b) shows the accuracy of DOA estimation for two and three simultaneous sources in terms of RMSE for different levels of additive noise (SNR). Figure 4 (c) illustrates single source DOA estimates in anechoic (0 ms) and reverberant (RT60=200ms) scenarios for different SNRs.

5. CONCLUSION

This paper proposes a co-prime circular microphone array for achieving a beampattern with a narrower main lobe and fewer side lobes than a conventional UCA with the same radius and numbers of microphones, while also avoiding spatial aliasing above the spatial Nyquist frequency of the UCA. Compared with a UCA with similar performance and the same spatial Nyquist frequency, the CPCMA significantly reduces the required number of array elements. Simulations also indicate advantages of the CPCMA in DOA estimation under high noise and low reverberation.

Future work will investigate the frequency-invariant performance of the CPCMA beamformer as well as more sophisticated DOA estimation algorithms based on real-world recordings and applications such as multi-source separation and enhancement.

6. REFERENCES

[1] Benesty, J., J. Chen, and Y. Huang, *Microphone Arrays Signal Processing*, Springer-Verlag, Berlin, Germany, 2008.

[2] Brandstein, M., and D. Ward, *Microphone Arrays: Signal Processing Techniques and Applications*, Springer-Verlag, Berlin, Germany, 2001.

[3] R. Levorato and E. Pagello, “DOA Acoustic Source Localization in Mobile Robot Sensor Networks,” *IEEE International Conference on Autonomous Robot Systems and Competitions*, pp. 71-76, 2015.

[4] M. Togami, A. Amano, T. Sumiyoshi, and Y. Obuchi, “DOA Estimation Method Based on Sparseness of Speech Sources for Human Symbiotic Robots,” *IEEE International Conference on Acoustics, Speech and Signal Processing*, pp. 3693-3696, 2009.

[5] M. Togami, S. Suganuma, Y. Kawaguchi, T. Hashimoto, and Y. Obuchi, “Transient Noise Reduction Controlled by DOA Estimation for Video Conferencing System,” *IEEE 13th International Symposium on Consumer Electronics*, pp. 26-29, 2009.

[6] M. Togami, “Multichannel Online Speech Dereverberation Under Noisy Environments,” *European Signal Processing Conference*, pp. 1078-1082, 2015.

[7] P. K. T. Wu, N. Epain, and C. Jin, “A Dereverberation Algorithm for Spherical Microphone Arrays Using Compressed Sensing Techniques,” *IEEE International Conference on Acoustics, Speech and Signal Processing*, pp. 4053-4056, March 2012.

[8] M. Zhang, S. Wu, W. Guo, and J. Ji. “A Microphone Array Dereverberation Algorithm Based on TF-GSC and Postfiltering,” *IEEE International Symposium on Broadband Multimedia Systems and Broadcasting*, pp. 1-4, 2016.

[9] E. A. P. Habets, J. Benesty, I. Cohen, and S. Gannot, “On a Tradeoff Between Dereverberation and Noise Reduction Using the MVDR Beamformer,” *IEEE International Conference on Acoustics, Speech and Signal Processing*, pp. 3741-3744, 2009.

[10] G. W. Elko, and A. N. Pong, “A Steerable and Variable First-Order Differential Microphone Array,” *IEEE International Conference on Acoustics, Speech and Signal Processing*, vol. 1, pp. 223-226, 1997.

[11] Benesty, J., J. Chen and I. Cohen, *Design of Circular Differential Microphone Arrays*, Springer International Publishing, Switzerland, 2015.

[12] G. Huang, J. Benesty, and J. Chen, “Design of Robust Concentric Circular Differential Microphone Arrays,” *Journal of Acoustical Society of America,* vol. 141, issue 5, pp. 3236-3249, May 2017.

[13] P. P. Vaidyanathan, and P. Pal, “Sparse Sensing with Coprime Arrays,” *the Forty-Fourth Asilomar Conference on Signals, Systems and Computers*, pp. 1405-1409, 2010.

[14] D. Bush, and N. Xiang, “Broadband Implementation of Coprime Linear Microphone Arrays for Direction of Arrival Estimation,” *Journal of the Acoustical Society of America*, vol. 138, issue 1, pp. 447-456, July 2015.

[15] D. Bush, and N. Xiang, “A Model-based Bayesian Framework for Sound Source Enumeration and Direction of Arrival Estimation Using A Coprime Microphone Array,” *22nd International Congress on Acoustics*, 2016.

[16] Q. Shen, W. Liu, W. Cui, S. Wu, Y. D. Zhang, and M. G. Amin, “Low-complexity Direction-of-arrival Estimation Based on Wideband Co-prime Arrays,” *IEEE/ACM Transactions on Audio, Speech, and Language Processing*, vol. 23, issue 9, pp. 1445-1456, 2015.

[17] J. Zhao, and C. Ritz, “Investigating Co-Prime Microphone Arrays for Speech Direction of Arrival Estimation,” *to be presented at the Asia-Pacific Signal and Information Processing Association Annual Summit and Conference (APSIPA 2018)*, November, 2018.

[18] Y. Liu, and J. R. Buck, “High-resolution Direction-of-Arrival Estimation in SNR and Snapshot Challenged Scenarios Using Multi-frequency Coprime Arrays,” 2017 *IEEE International Conference on Acoustics, Speech and Signal Processing*, pp. 3434-3438, 2017.

[19] H. Cox, R. Zeskind, and M. Owen, “Robust Adaptive Beamforming,” *IEEE Transactions on Acoustics, Speech, and Signal Processing*, vol. 35, issue 10, pp. 1365–1376, 1987.

[20] J. H. DiBiase, “A High-accuracy, Low-latency Technique for Talker Localization in Reverberant Environments Using Microphone Arrays,” *Brown University*, 2000.

[21] M. I. Mandel, R. J. Weiss, and D. P. W. Ellis, “Model-based Expectation-maximization Source Separation and Localization,” *IEEE Transactions on Audio, Speech, and Language Processing*, vol. 18, issue 2, pp. 382-394, 2010.

[22] S. Araki, H. Sawada, R. Mukai, and S. Makino, “Underdetermined Blind Sparse Source Separation for Arbitrarily Arranged Multiple Sensors," *Signal Processing*, vol. 87, pp. 1833-1847, 2007.

[23] B.W. Silverman, “Density Estimation for Statistics and Data Analysis,” *Monographs on Statistics and Applied Probability*, London: Chapman and Hall, 1986.

[24] X. Zheng, C. Ritz, and J. Xi, “Encoding and Communicating Navigable Speech Soundfields,” *Multimedia Tools and Applications*, vol. 75, pp. 5183-5204, 2016.

[25] J. Allen, and D. Berkley, “Image Method for Efficiently Simulating Small-room Acoustics,” *Journal of the Acoustical Society of America*, vol. 65, issue 4, pp. 943-950, April 1979.

[26] IEEE subcommittee on subjective measurements, “IEEE Recommended Practices for Speech Quality Measurements,” *IEEE Transactions on Audio and Electroacoustics*, vol. 17, pp. 227-46, 1969.

[27] Y. Hu and P. Loizou, “Subjective Evaluation and Comparison of Speech Enhancement Algorithms,” *Speech Communication*, vol.49, pp. 588-601, 2007.